Effects of Spectral Response Function (SRF) on Characterization of ATMS Bias

Lin Lin[1], Hu (Tiger) Yang[1], and Quanhua Liu[2]

[1] ESSIC, CICS-MD, College Park, Maryland, U.S.A.

[2] NOAA/NESDIS/Center for Satellite Application and Research, College Park, Maryland, U.S.A.

Introduction

Since 2012, the Advanced Technology Microwave Sounder (ATMS) data have been routinely assimilated into the global and regional forecast models at the world major numerical weather prediction (NWP) centers. The impacts from the ATMS data assimilation on global and regional forecasts are largely. As Joint Polar Satellite SysteM-1 (JPSS-1) will be launched soon in November 2017, it's necessary to estimate the impacts of both spectral response functions (SRFs) and antenna pattern on ATMS bias characterization, which is import for the data assimilation in NWP models. Previously, the accurate line-by-line Monochromatic Radiative Transfer Model (MonoRTM) is used to quantify the difference of simulated brightness temperature between boxcar SRFs and measured SRFs for S-NPP ATMS upper level temperature sounding channels 5-13. It is found that the difference has a magnitude of 0.3 K. In this study, JPSS-1 lab-measured SRFs and antenna patterns are investigated.

Evaluation of Imbalanced Spectral Response Functions (SRFs) on Brightness Temperature Simulations for ATMS Water Vapor Channels

- ATMS G-band channels 18-22 are located on a strong H_2O absorption line centered at 183 GHz frequency

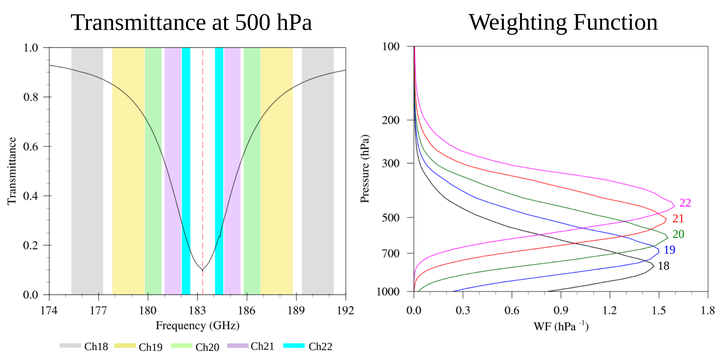

- JPSS-1 ATMS SRFs for channels 18 to 22 are provided by vendor in July, 2016
- Even though this dataset is outdated now, it's still of great value to evaluate the imbalance shown in the side-band channels 18-22 on brightness temperature simulations
- The dataset includes the flight mode (FM) filter digitized SRF data at base-plate temperature of 20°C and at primary local oscillator (LO) bias levels of G-band channels, which are used in the present study
- With the measured SRFs, the average gain difference between the lower- and higher-sideband, which is called as "imbalance" for each channel can be assessed
- To save computational time, the SRF is truncated at -20 dB to keep the 99% of the maximum SRF for each band of each channel

J1 ATMS G-Band SRFs (outdated)

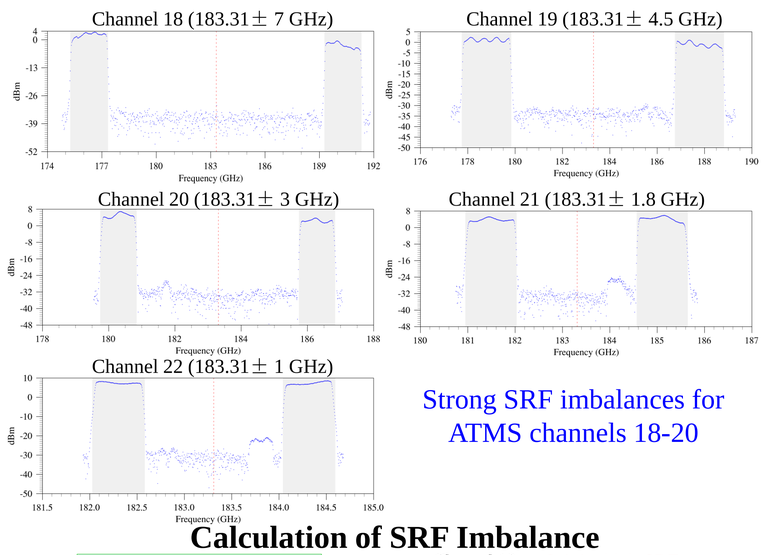

Strong SRF imbalances for ATMS channels 18-20

Calculation of SRF Imbalance

Original lab-measured SRF

↓

Truncate the SRF at -20 dB

↓

Compute average gain at each side band

$$\overline{G}_{low\ band} = \frac{\int_{f_1}^{f_2} G(f)\,df}{f_2 - f_1}$$

$$\overline{G}_{high\ band} = \frac{\int_{f_3}^{f_4} G(f)\,df}{f_4 - f_3}$$

↓

Compute the imbalance (unit: dB)

$$\Delta\overline{G} = \overline{G}_{low\ band} - \overline{G}_{high\ band}$$

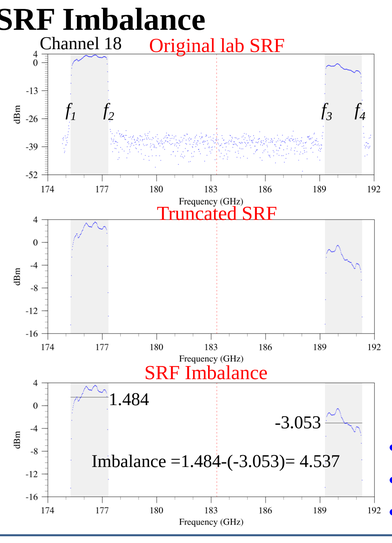

G-Band Channels SRF Imbalance				
18	19	20	21	22
4.537	1.997	2.419	-0.482	0.205

Four Scenarios for Removing SRF Imbalances

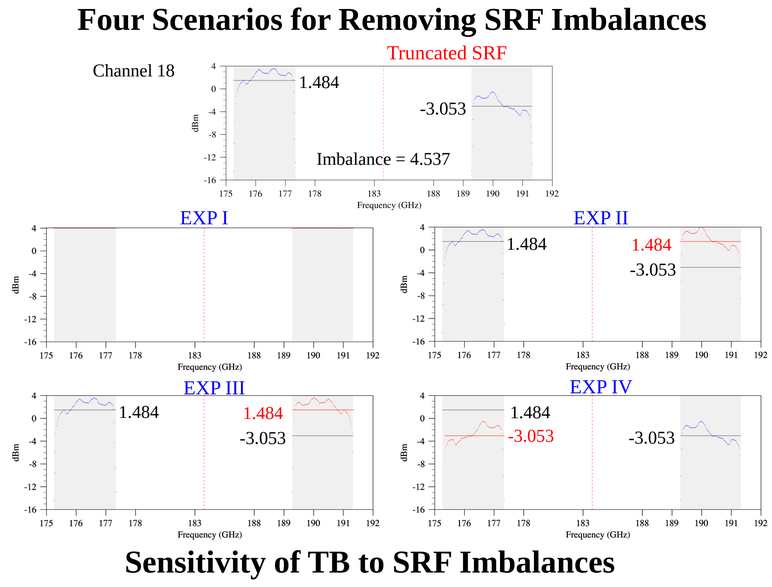

Sensitivity of TB to SRF Imbalances

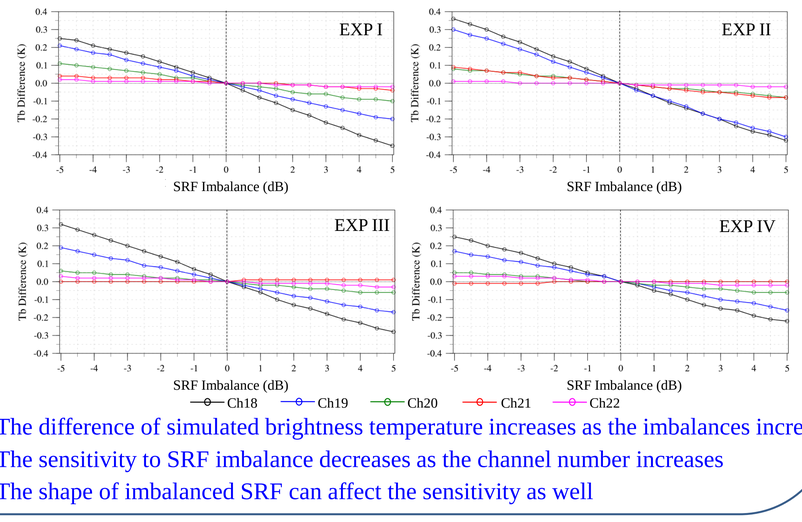

- The difference of simulated brightness temperature increases as the imbalances increase
- The sensitivity to SRF imbalance decreases as the channel number increases
- The shape of imbalanced SRF can affect the sensitivity as well

Comparison of BT Simulations Between Boxcar and Measured SRFs for JPSS-1

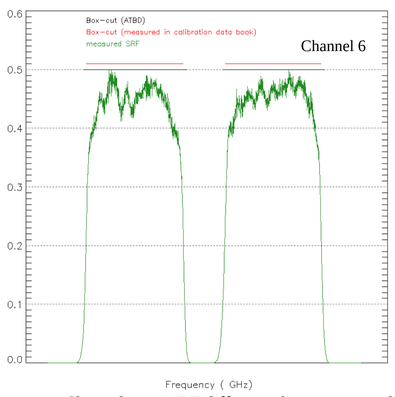

Table 1. CRTM J1 ATMS brightness temperature simulation difference in Kelvin between using SRF and box-cut (bc) for U.S. standard atmosphere over ozone at zenith angle = 50 and 0 degrees.

Channel Number	SRF, zenith=50°	bc-SRF	SRF, zenith=0°	bc-SRF
1	201.238	-0.046	156.151	0.047
2	193.671	0.006	149.121	0.008
3	229.126	0.029	219.352	0.033
4	249.615	0.110	240.735	0.117
5	254.349	-0.035	254.733	0.004
6	243.040	-0.300	251.142	-0.232
7	228.966	-0.016	236.682	-0.027
8	222.119	-0.050	227.361	-0.100
9	218.737	-0.002	221.206	-0.051
10	218.406	0.006	217.943	0.004
11	220.901	-0.006	219.763	-0.002
12	225.925	-0.096	224.038	-0.081
13	233.830	-0.085	230.882	-0.072
14	245.453	-0.127	241.401	-0.111
15	257.183	-0.009	253.309	-0.009
16	245.495	0.024	209.389	0.035
17	271.356	0.015	267.472	0.002
18	266.411	0.043	271.006	0.029
19	259.172	0.015	263.895	0.010
20	252.893	0.005	257.442	-0.000
21	245.926	0.065	250.222	0.072
22	240.043	0.014	244.297	0.018

Channels 1-17: BT difference between using boxcar (ATBD) and measured SRF
Channels 18-22: BT difference between using boxcar (ATBD) and boxcar (calibration book)

- Channel 6 shows the largest difference with the magnitude of ~0.3 K
- BT differences for other channels are within 0.13 K

Comparison of Antenna Patterns Between S-NPP and JPSS-1

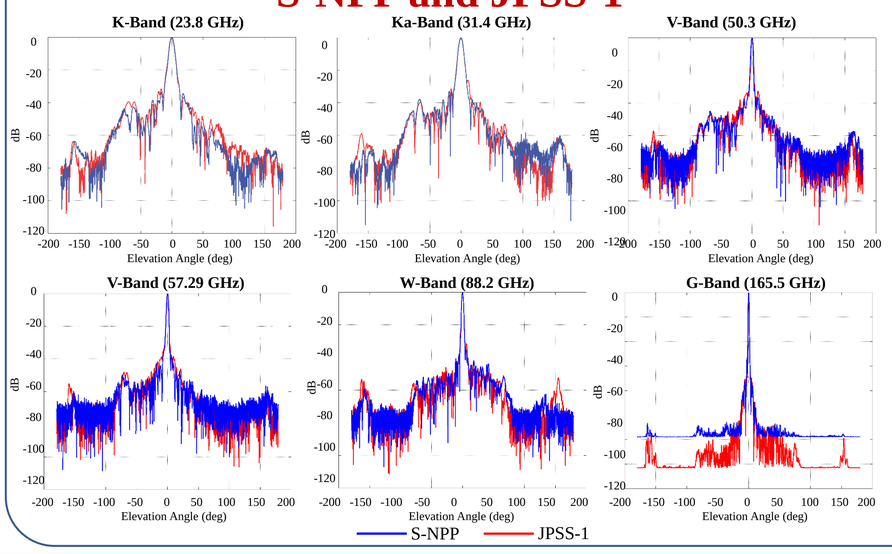

Comparison of Main Beam Efficiencies Between S-NPP and JPSS-1

ATMS Channel	η_{me}^{pp}		η_{me}^{pq}		ATMS Channel	η_{me}^{pp}		η_{me}^{pq}	
	S-NPP	JPSS-1	S-NPP	JPSS-1		S-NPP	JPSS-1	S-NPP	JPSS-1
1	0.9584	0.9598	0.0073	0.0086	12	0.9766	0.9756	0.0091	0.0079
2	0.9699	0.9702	0.0066	0.0064	13	0.9766	0.9756	0.0091	0.0079
3	0.9661	0.9631	0.0107	0.0102	14	0.9766	0.9756	0.0091	0.0079
4	0.9668	0.9684	0.0097	0.0097	15	0.9766	0.9756	0.0091	0.0079
5	0.9669	0.9714	0.0094	0.0101	16	0.9457	0.9597	0.0435	0.0365
6	0.9685	0.9729	0.0097	0.0092	17	0.8768	0.9394	0.0338	0.0395
7	0.9654	0.9690	0.0086	0.0090	18	0.8933	0.9389	0.0363	0.0340
8	0.9703	0.9724	0.0091	0.0087	19	0.8933	0.9389	0.0363	0.0340
9	0.9673	0.9714	0.0088	0.0086	20	0.8973	0.9360	0.0219	0.0318
10	0.9766	0.9756	0.0091	0.0079	21	0.8973	0.9360	0.0219	0.0318
11	0.9766	0.9756	0.0091	0.0079	22	0.8973	0.9360	0.0219	0.0318

J1 ATMS antenna has higher main beam efficiency in G-band channels compared to that of S-NPP ATMS, leading to better calibration accuracy for J1 ATMS G-band channels

Summary

- Both magnitude and shape of imbalanced SRFs are critical for brightness temperature simulations of water vapor channels
- It's suggested a necessity of providing the actual SRFs from all bands carefully measured by the instrument vendor to NWP users to build an accurate fast RTM for satellite data assimilation in NWP models
- Antenna efficiencies are required for ATMS TDR to SDR conversion
- G-band antenna beam efficiencies of J1 ATMS are much higher than those of S-NPP ATMS
- Detailed antenna pattern measurements are needed for the data assimilation when the spatial resolution of NWP model is higher than FOV